Smart Structures and Systems, *Vol. 22, No. 4 (2018) 469-479*
DOI: https://doi.org/10.12989/sss.2018.22.4.469

Weighted sum Pareto optimization of a three dimensional passenger vehicle suspension model using NSGA-II for ride comfort and ride safety

Mohammad Reza Bagheri[1], Masoud Mosayebi*[1], Asghar Mahdian[1] and Ahmad Keshavarzi[2]

[1]School of Mechanical Engineering, Malek-Ashtar University of Technology, ShahinShahr, Isfahan, Iran
[2]Department of Mechanical Engineering, Khomeinishahr Branch, Islamic Azad University, Isfahan, Iran

(Received August 3, 2018, Revised September 17, 2018, Accepted September 20, 2018)

Abstract. The present research study utilizes a multi-objective optimization method for Pareto optimization of an eight-degree of freedom full vehicle vibration model, adopting a non-dominated sorting genetic algorithm II (NSGA-II). In this research, a full set of ride comfort as well as ride safety parameters are considered as objective functions. These objective functions are divided in to two groups (ride comfort group and ride safety group) where the ones in one group are in conflict with those in the other. Also, in this research, a special optimizing technique and combinational method consisting of weighted sum method and Pareto optimization are applied to transform Pareto double-objective optimization to Pareto full-objective optimization which can simultaneously minimize all objectives. Using this technique, the full set of ride parameters of three dimensional vehicle model are minimizing simultaneously. In derived Pareto front, unique trade-off design points can selected which are non-dominated solutions of optimizing the weighted sum comfort parameters versus weighted sum safety parameters. The comparison of the obtained results with those reported in the literature, demonstrates the distinction and comprehensiveness of the results arrived in the present study.

Keywords: full vehicle vibration model; multi-objective optimization; non-dominated sorting genetic algorithm II; passenger vehicle suspension model; weighted sum Pareto optimization

1. Introduction

Vehicle suspension systems can play the role of a dynamic system and simulate the response of the vehicle to various inputs and disturbances using vehicle properties. Suspension system isolates chassis and passengers from the roughness of the road to provide a more comfortable ride. Ride comfort is mainly affected by vehicle properties located in suspension system. Researchers have conducted several studies on suspension to improve the vehicle ride comfort. Uys *et al.* (2007) have surveyed the ride comfort of off-road vehicles and correspond optimal suspension. Tong and Guo (2012), while considering vehicle ride comfort, built a new type of suspension to even the vertical loads of each wheel. Chen *et al.* (2013) applied the grey relational analysis and Taguchi method on the vehicle noise and vibration domain and showed improvement in vehicle vibration performance.

Furthermore, the vehicle vibration can bring about driver’s fatigue (ride comfort), it also decreases in driving safety and vehicle operation stability (ride safety). Hence, designers in automotive industry try to improve suspension systems considering all ride parameters. Two principal parameters are sprung mass acceleration (Ihsan *et al.* 2008), determining ride comfort, and suspension deflection (Gündoğdu 2007), indicating the limit of the vehicle body motion. Another performance measure, also significantly important, is the dynamic tire load applied on the pavement (Zhang *et al.* 2013). Since the passive suspension system is formed by springs and dampers with fixed rates with serious limitations, this cannot efficiently affect a compromise between ride comfort and ride safety. Therefore, the goals set by vehicle suspension system researchers in finding optimum suspension systems are to compromise between ride parameters.

Researchers have applied various methods on different vehicle models. Vehicle models such as two-DOF, quarter vehicle, four or six-DOF, half vehicle, or seven-DOF full vehicle models. They use analytical methods where a linear vehicle model is investigated by solving linear ordinary differential equations. Because of simplicity, quarter vehicle models are mostly preferred. Liang *et al.* (2013) considered a quarter vehicle model to design an optimal vibration controller in order to prolong the working life of suspension system and improve ride comfort. Since the quarter vehicle model is insufficient to provide information on the angular motions of a vehicle, some researchers utilized more complex models like half and full vehicle models. These models supply information about the pitch, roll and bounce motions of a vehicle body. Barbosa (2011) applied a half vehicle dynamic model and spectral method to obtain the frequency response of the model to a measured pavement roughness. Jin *et al.* (2016) considered an 11 degrees of freedom of vehicle model to study the influence of ratio between unsprung and sprung mass on ride comfort of vehicles driven by in-wheel motors. Mahmoodabadi *et al.* (2018) applied weighted sum method to optimize multiple objective functions of two- and five-DOF vehicle vibration models.

*Corresponding author, Ph.D.
E-mail: m.mosayebi@mut-es.ac.ir

http://www.techno-press.com/journals/sss&subpage=7
ISSN: 1738-1584 (Print), 1738-1991 (Online)

Genetic algorithms represent an intelligent exploitation of a random search based on the evolutionary ideas of natural selection and genetics used to solve optimization problems. Optimization problems in engineering are first formulated as mathematical models consisting of functions which provide optimal system performance and then attempts are made to optimize the model or the function components. The idea behind a genetic algorithm is using optimization strategies known as Darwinian Evolution, efficiently and successfully, and transforming to mathematical form. Hada *et al.* (2007) applied genetic algorithm to achieve an optimum trade off among ride comfort, handling quality, and suspension stroke simultaneously for random input. Seifi *et al.* (2015) optimized full vehicle model using genetic algorithm to improve the ride comfort, road holding, workspace and preventing rollover.

In order to solve mathematical optimization problems involving more than one objective function to be optimized simultaneously, several modeling methods have been developed in solving multi-objective optimization problem (MOOP). Costas *et al.* (2014) applied a surrogate-based multi-objective optimization to a crash-worthiness problem of a frontal crash absorber. Busch *et al.* (2014) considered an active all-wheel-steering car and formulated Model-based objectives and summarized in a multi-objective optimization problem, then achieved unconstrained problem by defining a penalty function. Li *et al.* (2018) presented a multi-objective optimization control method of active suspension system for solving the negative vibration issues, and derived Pareto solution set of optimal parameters. Gu *et al.* (2013) combined a Kriging model and a Non-dominated sorting genetic algorithm II (NSGA-II) for MOOP of design for vehicle occupant restraint system under frontal crash, and obtained some enhanced results compared with the original design. Shojaeefard *et al.* (2017) investigated the optimal design of suspension system using NSGA-II and technique for order of preference by similarity to ideal solution.

In the present research, our main contribution as follow: a Pareto optimization method based on a Non-dominated sorting genetic algorithm II (NSGA-II) is provided and applied on a full vehicle model. In this full vehicle model having eight-DOFs, vertical movement of passenger seat, vehicle body and four tires are considered. Furthermore, in this three dimensional model, pitch acceleration, and roll acceleration of vehicle body are dealt with. Using the presented method, full set of ride comfort and ride safety parameters of the vehicle (passenger seat acceleration, vehicle body pitch acceleration, vehicle body roll acceleration, dynamic tire forces, tire velocity, and suspension deflections), which are in conflict with others, are considered simultaneously. Also, a special optimization technique is used to minimize all ride parameters with Pareto optimization. Using weighted sum method in this technique, the Pareto double-objective optimization is transformed to Pareto full-objective optimization which can minimize all objectives, simultaneously. Moreover, road profile considered in the form of step function makes optimal points independent of excitation frequency. Then, the trade-off design points correspond to ride parameters are defined and the optimum suspension parameters are derived.

2. Optimization methods and Non-dominated sorting genetic algorithm II

There are several optimization methods, finding intended optimal design parameters and satisfying certain constraints, to minimize or maximize the value of desired objective function. Usually, a single-objective optimization problem can be mathematically described as follows (Lin *et al.* 2018)

Find the vector

$$\mathbf{X} = [x_1, x_2, \ldots, x_n]^T, \tag{1}$$

to minimize or maximize objective function

$$F(\mathbf{X}) = F(x_1, x_2, \ldots, x_n), \tag{2}$$

subject to constraints

$$g_j(\mathbf{X}) \le 0, \quad j = 1, 2, \ldots, m, \tag{3}$$

$$x_{kl} \le x_k \le x_{ku}, \quad k = 1, 2, \ldots, n, \tag{4}$$

here $\boldsymbol{X} \in \Re^n$ is the vector of design variables, $\boldsymbol{F(X)}$ is the objective function, which must be minimized or maximized, $g_j(\boldsymbol{X})$ is the j-th constraint function, and the last set of constraints in Eq. (4) are variable bound constraints, where restrict value of each variable x_k to get a value between a lower bound x_{kl} and an upper bound x_{ku}, in optimization process.

In multi-objective optimization problem (MOOP), a number of objective functions are to be minimized or maximized. Therefore, the multi-objective optimization has similar mathematical form as single-objective optimization, with the difference that in Eq. (2), objective function vector is defined as follows (Lin *et al.* 2018)

$$\mathbf{F}(\mathbf{X}) = [f_1(\mathbf{X}), f_2(\mathbf{X}), \ldots, f_p(\mathbf{X})]^T, \tag{5}$$

where$\boldsymbol{F(X)} \in \Re^p$ is the vector of objective functions, which must minimized or maximized and $f_q(x)$, $q=1,2,\ldots,p$ is q-th objective function.

Weighted sum method is used in multi-objective optimization to optimize a number of objective functions simultaneously. In this method, an aggregated objective function is obtained by multiplying each objective function by a weighting factor and then summing up all weighted objective functions as follows (Deb 2001)

$$f(\mathbf{X})_{WS} = \frac{w_1}{s_1} f_1(\mathbf{X}) + \frac{w_2}{s_2} f_2(\mathbf{X}) + \ldots + \frac{w_p}{s_p} f_p(\mathbf{X}), \tag{6}$$

where w_q $(q=1,2,\ldots,p)$ is a weighting factor and s_q $(q=1,2,\ldots,p)$ is a scaling factor for the q-th objective function.

In Pareto optimization, **Pareto domination** concept is used to compare any of the two solutions to each other. It can be described as a vector $\boldsymbol{R}=[r_1,r_2,\ldots,r_p]^T \in \Re^p$ similar Eq. (5), is dominate to vector $\boldsymbol{S}=[s_1,s_2,\ldots,s_p]^T \in \Re^p$, if there is at least one r_q $(q=1,2,\ldots,p)$ which is smaller than s_q $(q=1,2,\ldots,p)$, the remaining *r*s are either smaller or equal to corresponding *s*s. The **Pareto optimality** concept can be defined as the solution with vector $\boldsymbol{X}^0$ is Pareto optimal (minimal), if no other solution can be found to dominate to $\boldsymbol{F}(\boldsymbol{X}^0)$ using the definition of Pareto domination concept. The concept of **Pareto set** can be defined as; a Pareto set is a set consisting of all the Pareto optimal vectors such as $\boldsymbol{X}^0$where there is no other vector $\boldsymbol{X}$ that $\boldsymbol{F}(\boldsymbol{X})$ dominate any $\boldsymbol{F}(\boldsymbol{X}^0)$ correspond to $\boldsymbol{X}^0$in Pareto set. In other words, the Pareto set is a set of the vectors of design variables with dominated vectors of objective functions, where vectors of objective functions non-dominate with themselves. Also, The **Pareto front** concept can be defined as; a Pareto front is a set of vector such as $\boldsymbol{F}(\boldsymbol{X}^0)$, which are obtained using the vectors $\boldsymbol{X}^0$in the Pareto set. In other words, the Pareto front is a set of the dominated vectors of objective functions that non-dominate with themselves. Since, in Pareto optimization, it is almost impossible to obtain a single solution to optimize all objectives simultaneously and finding corresponding objective function vector of one solution which dominates other ones is difficult; therefore, Pareto optimal solutions (non-dominated solutions of all possible solutions in its solution space) are the desired solution.

Non-dominated sorting genetic algorithm is a multi-objective optimization algorithm and is an instance of an evolutionary optimization algorithm which is an extended form of the genetic algorithm (Sedighizadeh *et al.* 2014). NSGA is an extension of the genetic algorithm for multi-objective function optimization. The algorithm uses an evolutionary process including normal selection, genetic crossover, and genetic mutation, as being in genetic algorithm. In addition, integral parts of NSGA-II are fast ranking of non-dominated solutions, crowding distance and elitist strategy (Bharti *et al.* 2012). The main steps of the NSGA- II are provided below:
Step 1. Initialize a population randomly.
Step 2. Implement the multi-objective operation, consist of non-dominated sorting, crowding distance calculation and sorting the solutions.
Step 3. Start main loop.
Step 4. Generate offspring from crossover method.
Step 5. Generate offspring from mutation method.
Step 6. Aggregate the parents and offspring.
Step 7.Same operation in Step 2.
Step 8. Select the fittest solutions.
Step 9.Same operation in Step 2.
Step 10. Return to Step 3 and repeat the algorithm until establishing stopping condition.

3. Mathematical model

An eight-DOF vehicle model is considered in this study as is shown in Fig. 1. The model consists of one passenger seat and sprung mass that is supported on springs and unsprung masses which refer to the mass of wheel assembly. The model considers heave, pitch and roll of the sprung mass and vertical motions of the four unsprung masses and passenger seat. The suspension, tire, passenger seat are modeled by linear springs in parallel with dampers. Parameters m_s, m_1, m_2, m_3, m_4, m_p, I_x and I_y, are expressed as sprung mass, front right tire mass, front left tire mass, rear right tire mass, rear left tire mass, seat mass, pitch moment of inertia of sprung mass and roll moment of inertia of sprung mass, respectively. Parameters k_i, c_i, k_{ti}, c_{ti}, k_p and c_p, where $i=1,2,3,4$, denote spring and damping coefficient of suspension, spring and damping coefficient of tire and spring and damping coefficient of passenger seat, respectively.

Using the Newton's second law of motion, the following equations of motion for sprung mass, unsprung masses and passenger seat are derived.

$$\begin{aligned} & m_s \ddot{\delta}_0 + \sum_{i=1}^{4} \Big\{ k_i \big[\delta_0 + (y_i - y_0)\theta_0 + (x_0 - x_i)\phi_0 - \delta_i \big] \\ & \quad + c_i \Big[\dot{\delta}_0 + (y_i - y_0)\dot{\theta}_0 + (x_0 - x_i)\dot{\phi}_0 - \dot{\delta}_i \Big] \Big\} \\ & \quad + k_p \big[\delta_0 + (y_p - y_0)\theta_0 + (x_0 - x_p)\phi_0 - \delta_p \big] \\ & \quad + c_p \Big[\dot{\delta}_0 + (y_p - y_0)\dot{\theta}_0 + (x_0 - x_p)\dot{\phi}_0 - \dot{\delta}_p \Big] = 0 \end{aligned} \tag{7}$$

$$\begin{aligned} & I_x \ddot{\theta}_0 + \sum_{i=1}^{4} \Big\{ k_i (y_i - y_0) \big[\delta_0 + (y_i - y_0)\theta_0 + (x_0 - x_i)\phi_0 - \delta_i \big] \\ & \quad + c_i (y_i - y_0) \Big[\dot{\delta}_0 + (y_i - y_0)\dot{\theta}_0 + (x_0 - x_i)\dot{\phi}_0 - \dot{\delta}_i \Big] \Big\} \\ & \quad + k_p (y_p - y_0) \big[\delta_0 + (y_p - y_0)\theta_0 + (x_0 - x_p)\phi_0 - \delta_p \big] \\ & \quad + c_p (y_p - y_0) \Big[\dot{\delta}_0 + (y_p - y_0)\dot{\theta}_0 + (x_0 - x_p)\dot{\phi}_0 - \dot{\delta}_p \Big] = 0 \end{aligned} \tag{8}$$

$$\begin{aligned} & I_y \ddot{\phi}_0 + \sum_{i=1}^{4} \Big\{ k_i (x_0 - x_i) \big[\delta_0 + (y_i - y_0)\theta_0 + (x_0 - x_i)\phi_0 - \delta_i \big] \\ & \quad + c_i (x_0 - x_i) \Big[\dot{\delta}_0 + (y_i - y_0)\dot{\theta}_0 + (x_0 - x_i)\dot{\phi}_0 - \dot{\delta}_i \Big] \Big\} \\ & \quad + k_p (x_0 - x_p) \big[\delta_0 + (y_p - y_0)\theta_0 + (x_0 - x_p)\phi_0 - \delta_p \big] \\ & \quad + c_p (x_0 - x_p) \Big[\dot{\delta}_0 + (y_p - y_0)\dot{\theta}_0 + (x_0 - x_p)\dot{\phi}_0 - \dot{\delta}_p \Big] = 0 \end{aligned} \tag{9}$$

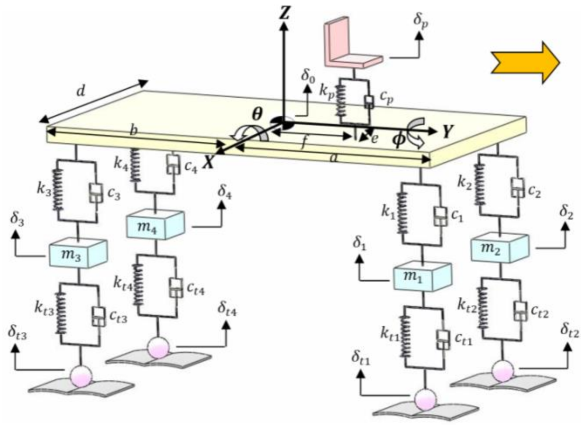

Fig. 1 Full vehicle model

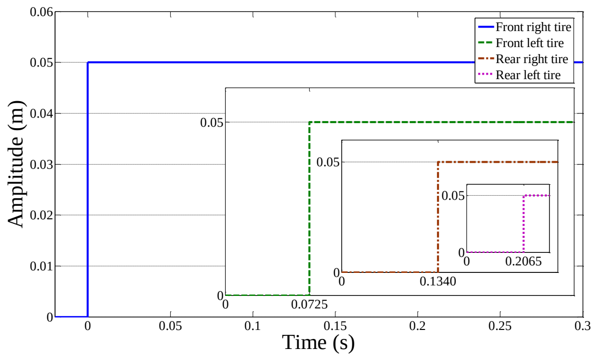

Fig. 2 Excitation shape created by step function road profile

$$\begin{aligned} & m_i \ddot{\delta}_i + [k_i + k_{ti}]\delta_i - k_i[\delta_0 + (y_i - y_0)\theta_0 + (x_0 - x_i)\phi_0] - k_{ti}\delta_{ti} \\ & + [c_i + c_{ti}]\dot{\delta}_i - c_i\left[\dot{\delta}_0 + (y_i - y_0)\dot{\theta}_0 + (x_0 - x_i)\dot{\phi}_0\right] - c_{ti}\dot{\delta}_{ti} = 0 \quad (10) \\ & \qquad where \quad i = 1,2,3,4 \end{aligned}$$

$$\begin{aligned} & m_p \ddot{\delta}_p - k_p[\delta_0 + (y_p - y_0)\theta_0 + (x_0 - x_p)\phi_0 - \delta_p] \\ & - c_p\left[\dot{\delta}_0 + (y_p - y_0)\dot{\theta}_0 + (x_0 - x_p)\dot{\phi}_0 - \dot{\delta}_p\right] = 0 \end{aligned} \quad (11)$$

Where δ_0, θ_0 and ϕ_0 are sprung mass heave, pitch and roll, respectively, and δ_i and δ_p are vertical movement of *i*-th unsprung mass and passenger seat, respectively. Moreover $(x_i$-$x_0)$ and $(y_i$-$y_0)$, are distance between *i*-th unsprung mass connection point to sprung mass and center of gravity of sprung mass, on x and y direction, respectively, and $(x_p$-$x_0)$ and $(y_p$-$y_0)$ are distance between passenger seat connection point to sprung mass and center of gravity of sprung mass, on x and y direction, respectively.

The dynamic model is excited by a step function while height *h=0.05 m* and vehicle velocity *v=20 m/s* are utilized for the analysis. The road profile illustrated in Fig. 2. The right and left sides have same road profile amplitude but there is a time delay of *d/v* and also the rear wheel will follow the same trajectory as the front wheels with a time delay of *(a+b)/v*. This road input will help excite bounce, pitch and roll motion of vehicle body simultaneously. Also the road profile in the form of step function causing optimum points are independent of excitation frequency of road profile, where are explaining as follows.

4. Objective functions

To improve the ride comfort and ride safety, nearly in most works in this field, the vehicle is optimized to decrease two major parameters: passenger seat acceleration (SA) and dynamic tire force (TF), respectively. In the present research, while considering the full vehicle model, body pitch acceleration (PA), body roll acceleration (RA), tire velocity (TV) and suspension deflection (SD), are also included for objective functions. The objective functions are divided in two groups: the first group includes SA, PA and RA (ride comfort group) minimized to improve the ride comfort and the second group comprises TF, TV and SD (ride safety group) minimized to improve ride safety.

In optimization process, the maximum absolute value of objective functions at time response have been considered as value of objective function. Therefore, the objective functions in Eq. (5) are defined as follows:

SA: minimization of maximum absolute value of passenger seat acceleration

$$f_1(X) = f_{SA}(X) = \max\left|\ddot{\delta}_p\right| \quad (12)$$

PA: minimization of maximum absolute value of body pitch acceleration

$$f_2(X) = f_{PA}(X) = \max\left|\ddot{\theta}_0\right| \quad (13)$$

RA: minimization of maximum absolute value of body roll acceleration

$$f_3(X) = f_{RA}(X) = \max\left|\ddot{\phi}_0\right| \quad (14)$$

Since each wheel has a different performance, the values for the objective functions in ride safety group naturally become different. To present the value of the objective functions in ride safety group (TF, TV and SD) for whole vehicle, the sum value of maximum absolute of objective functions in wheels are setting at the objective function value, as follows

$$F = \sum_{i=1}^{4} \max|F_i|, \; i = 1,2,3,4, \quad (15)$$

where F and F_i *(i=1,2,3,4)* are objective function of whole vehicle and each wheel, respectively. Therefore:

TF: minimization of maximum absolute value of dynamic tire force

$$f_4(X) = f_{TF}(X) = \sum_{i=1}^{4} \max|TF_i|,$$

$$where\ TF_i = \left[k_{ti}(\delta_{ti} - \delta_i) + c_{ti}\left(\dot{\delta}_{ti} - \dot{\delta}_i \right) \right]\ and\ i = 1,2,3,4 \tag{16}$$

TV: minimization of maximum absolute value of tire velocity

$$f_5(X) = f_{TV}(X) = \sum_{i=1}^{4} \max|TV_i|,$$

$$where\ TV_i = \left[\dot{\delta}_i \right]\ and\ i = 1,2,3,4 \tag{17}$$

SD: minimization of maximum absolute value of suspension deflection

$$f_6(X) = f_{SD}(X) = \sum_{i=1}^{4} \max|SD_i|,$$

$$where\ SD_i = \left[\delta_0 + (y_i - y_0)\theta_0 + (x_0 - x_i)\phi_0 - \delta_i \right],\ and\ i = 1,2,3,4 \tag{18}$$

Study shows that the two objective groups are in conflict. That is, these two objective groups cannot simultaneously generate higher levels of performance. Therefore, a Pareto optimization is needed to obtain a good trade-off. A Pareto solution will be obtained, and designers can select an effective design point from the solution set to satisfy different needs.

5. Design variables and constraints

A number of factors influence dynamic characteristic of vehicle and passenger seat. Some of these common factors are seat spring stiffness, seat damper coefficient, suspension spring stiffness, suspension damper coefficient, wheel mass and tire parameters.

Most design variables have a converse influence on different objectives, that is, an improvement in one objective sacrifices another one. However, there are still some ways to find a compromise between these conflicting objectives. The present research adopts NSGA-II to optimize this latter problem. Table 1 provides a list of fixed parameters utilized in the analysis (Panzade 2005), and Table 2 gives the design variables and the corresponding lower and upper bounds (Panzade 2005).

The constraints in Pareto optimization problem are variable bound constraints according to Eq. (4). With considering Table 2, constraints are defined as follows

$$\begin{cases} 75000N/m \le k_1 = k_2 \le 100000N/m \\ 875N.s/m \le c_1 = c_2 \le 3000N.s/m \\ 32000N/m \le k_3 = k_4 \le 70000N/m \\ 875N.s/m \le c_3 = c_4 \le 3000N.s/m \\ 90000N/m \le k_p \le 120000N/m \\ 400N.s/m \le c_p \le 900N.s/m \end{cases} \tag{19}$$

Table 1 Fixed parameters (Panzade 2005)

Fixed parameters	Values	Fixed parameters	Values
$d\,(m)$	1.450	$m_1 = m_2\,(kg)$	85
$a\,(m)$	1.524	$m_3 = m_4\,(kg)$	60
$b\,(m)$	1.156	$k_t\,(N/m)$	200000
$m_s\,(kg)$	2160	$c_t\,(N.s/m)$	0
$I_x\,(kg.m^2)$	4140	$e\,(m)$	0.375
$I_y\,(kg.m^2)$	946	$f\,(m)$	0.234
$m_p\,(kg)$	100		

Table 2 Design variable ranges (Panzade 2005)

Design variables	Lower value	Upper value
$k_1 = k_2\,(N/m)$	75000	100000
$c_1 = c_2\,(N.s/m)$	875	3000
$k_3 = k_4\,(N/m)$	32000	70000
$c_3 = c_4\,(N.s/m)$	875	3000
$k_p\,(N/m)$	90000	120000
$c_p\,(N.s/m)$	400	900

6. Analysis and results

A Non-dominated sorting genetic algorithm II (NSGA-II) introduced in the previous sections is employed for multi-objective design of full vehicle model which is shown in Fig. 1. Between various possible pairs of objectives in two conflicting groups (ride comfort and ride safety group), five different pairs are considered in the Pareto double-objective optimization processes. Pairs of objectives to be optimized separately are (SA,TF), (SA,TV), (SA,SD), (PA,TF) and (RA,TF). A population of 200 individuals with a crossover probability of 0.7 and a mutation probability of 0.3 are utilized. Pareto fronts of each chosen pair are displayed in Figs. 3-7. As is observed by studying this figures, obtaining a better value for one objective would normally cause a worse value for another objective.

Fig. 3 depicts the Pareto front of seat acceleration and dynamic tire force representing different non-dominated optimum points with respect to the conflicting objectives. The diamond dots are Pareto front points. The Pareto front provides a set of application solutions. Any point in the Pareto front can be a solution. In this figure, points X_1 and Y_1 stand for the best seat acceleration and the best dynamic tire force, respectively. It should be noted that all the optimum design points in this Pareto fronts are non-dominated and can be chosen by a designer. As the figure clearly shows choosing a better value for any objective function in these Pareto fronts would cause a worse value of another objective function. Obviously, there are some important optimal design facts between these objective functions that can be observed readily in that Pareto front.

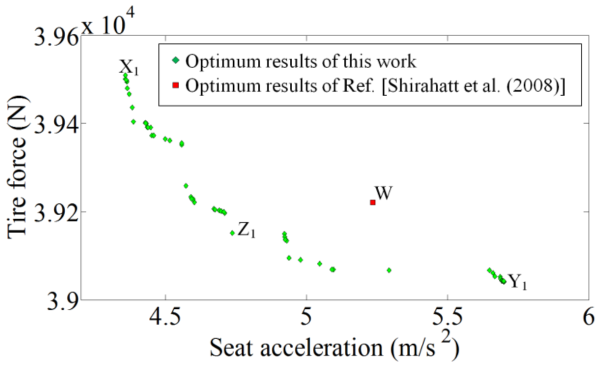

Fig. 3 Pareto front for seat acceleration and dynamic tire force

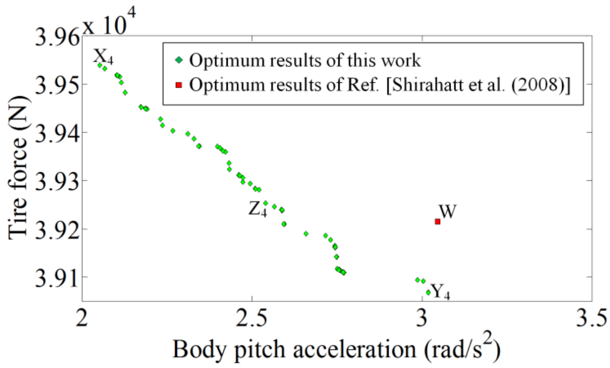

Fig. 6 Pareto front for body pitch acceleration and dynamic tire force

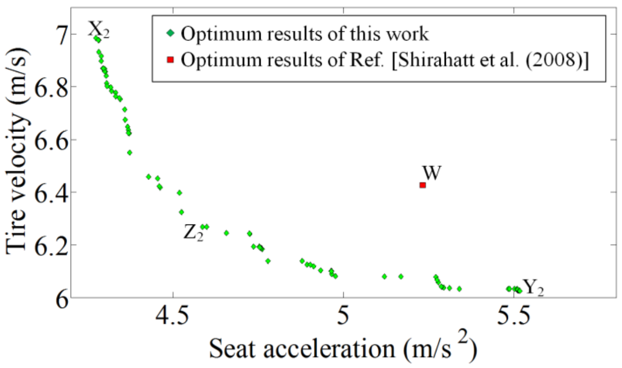

Fig. 4 Pareto front for seat acceleration and tire velocity

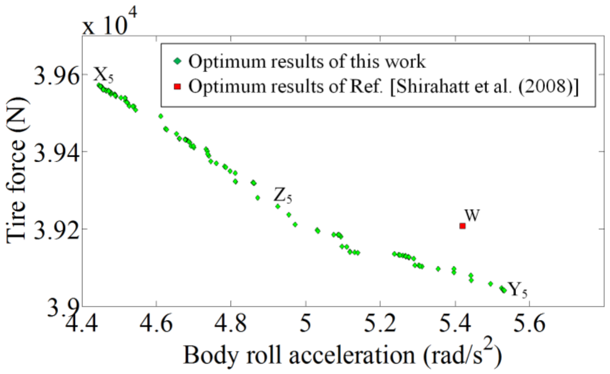

Fig. 7 Pareto front for body roll acceleration and dynamic tire force

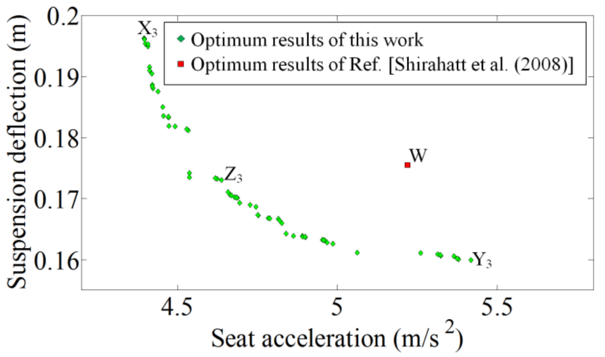

Fig. 5 Pareto front for seat acceleration and suspension deflection

In Fig. 3, point Z_1 is the point which demonstrates an important optimal design fact. Optimum design point Z_1 obtained in the present research exhibits a small increase in dynamic tire force in comparison with that of point Y_1 (the design with the least dynamic tire force) whilst its seat acceleration improves considerably. In fact, the trade-off design point Z_1, would not have been obtained without the application of the Pareto optimum approach presented in this study.

Also Fig. 3 demonstrates the optimum point *W* obtained from optimum design variables derived by Shirahatt *et al.* (2008). An eight-DOF passenger vehicle model has been considered by Shirahatt *et al.* (2008) and a single-objective optimization method has been applied to obtain the optimum suspension parameters to improve the ride comfort of vehicle model. Also, the genetic algorithm has been used to solve the problem, and the results have been compared to those obtained by simulated annealing technique. The optimum point *W* has been obtained from the results derived by genetic algorithm method. Fig. 3 displays the fact that optimum points in Pareto front have improved objective values than point *W*.

Such non-dominated Pareto fronts of the other chosen sets of objective functions are shown in Figs. 4-7. Design points X_2 and X_3 stand for the best SA and points X_4 and X_5 stand for the best PA and RA, respectively, whilst points Y_2 and Y_3 represent the best TV and SD, respectively, and points Y_4 and Y_5 represent the best TF. Similarly, the trade-off design points Z_2, Z_3, Z_4 and Z_5 are those which demonstrate the important optimal design fact. In Figs. 3-5, the value of seat accelerations is improved about 17%, 17% and 14% from points Y_1 to Z_1, Y_2 to Z_2 and Y_3 to Z_3, respectively, although other objective functions increase small. Also, in Figs. 6 and 7, the values of body pitch accelerations and body roll accelerations improve about

16%and 11% from points Y_4 to Z_4 and Y_5 to Z_5, respectively.

The derived optimum design points and corresponding values of objective functions and design variables related to these points and point W are listed in Table 3, where F_1 and F_2 are values of first and second objective function, corresponding with these points, respectively. The highlighted values in Table 3 are minimum optimum values of objective functions which has been used for obtaining the normalized objectives in ride comfort group and ride safety group, where are explaining as follows.

The corresponding values of objective functions of the optimum point *W* (obtained by Shirahatt *et al.* (2008)) are also given in Table 4.

A special optimization technique is applied to minimize all vehicle ride parameters by Pareto optimization, simultaneously. In this technique, in each group, all objective function is converted to one aggregate objective function by weighted sum method according to Eq. (6) as follows

$$\begin{aligned} f_{SNC}(X) &= f_{SA}(X)/ f_{SA}(X)_{\min} + f_{PA}(X)/ f_{PA}(X)_{\min} \\ &\quad + f_{RA}(X)/ f_{RA}(X)_{\min}, \\ f_{SNS}(X) &= f_{TF}(X)/ f_{TF}(X)_{\min} + f_{TV}(X)/ f_{TV}(X)_{\min} \\ &\quad + f_{SD}(X)/ f_{SD}(X)_{\min}, \end{aligned} \tag{20}$$

where $f_q(X)$ $(q=SA,...,SD)$ are objective functions in Eqs. (12)-(18) and $f_q(X)min$ $(q=SA,...,SD)$ are minimum optimum values of objective functions which have been derived in the previous Pareto double-objective optimization for the five pair objective function. Minimum derived values in the Pareto double-objective optimization for the five pair objective function have been highlighted in Table 3. The $f_{SNC}(X)$ and $f_{SNS}(X)$ are aggregate objective functions of ride comfort group and ride safety group which are said to SNC and SNS, respectively. Here with selecting weighting factor $w_q=1$ $(q=SA,...,SD)$, the weight of all objective functions are equal and with selecting scaling factor $s_q=f_q(X)_{min}$ $(q=SA,...,SD)$, all objective functions are being normalized with their minimum optimum values. In this regard, SNC and SNS are said to be **summation** of **normalized** objectives in ride **comfort** group and ride **safety** group, respectively. In this section, a Pareto solution is derived by minimizing two aggregate objective function (SNC, SNS). Actually, by mentioned technique, the Pareto double-objective optimization is transformed to Pareto full-objective optimization and six objective function are optimizing by this weighted sum Pareto optimization method, simultaneously.

Non-dominated Pareto fronts of summation of normalized objectives in ride comfort group and ride safety group (SNC, SNS) are displayed in Fig. 8. It is observed in this Figure that obtaining a better value for one aggregate objective would normally cause a worse value for another aggregate objective. Also points X_6 and Y_6 stand for the best summation of normalized objectives in ride comfort group and ride safety group, respectively. Similarly, the trade-off design point Z_6 are those which demonstrate the important optimal design fact. In Fig. 8, the value of summation of normalized objectives in ride comfort group improve about 9% from points Y_6 to Z_6, although summation of normalized objectives in ride safety group increase small. Also, the optimum points corresponding to the previous Pareto double-objective optimization for the five pair objective functions are illustrated in Fig. 8. As can be observed, points in Pareto front are dominated to previous derived optimum points and point *W*.

With selecting unequal values for weighting factors w_q $(q=SA,...,SD)$, various weights for objective functions are selected and the weighted sum Pareto optimization can optimize ride parameters of three dimensional vehicle model with different weights, simultaneously.

The time behavior of the seat acceleration corresponding to optimum value of point Z_1along with optimum point *W* proposed in Shirahatt *et al.* (2008) are shown for the sake of comparison in Fig. 9.

This figure clearly indicates that the obtained values of seat acceleration derived via the design point Z_1 in the present research are better than those derived via the design point *W* given in Shirahatt *et al.* (2008). In addition, the superiority of other optimum points in this research relative to point *W* can be shown. The maximum absolute value of seat accelerations corresponding to optimum points *W*, Z_1, Z_2, ..., Z_6 and their improvement percentage than the maximum absolute value of seat accelerations of point *W* are given in Table 5.

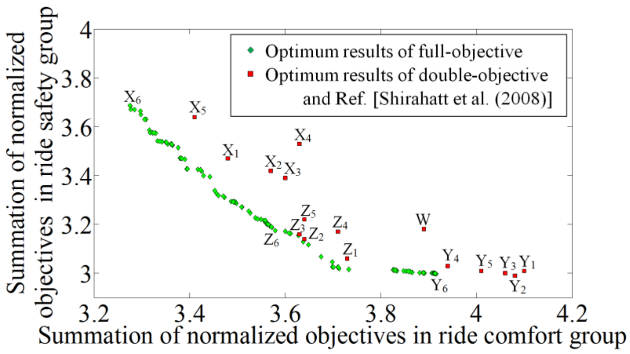

Fig. 8 Pareto front for summation of normalized objectives in ride comfort group and ride safety group

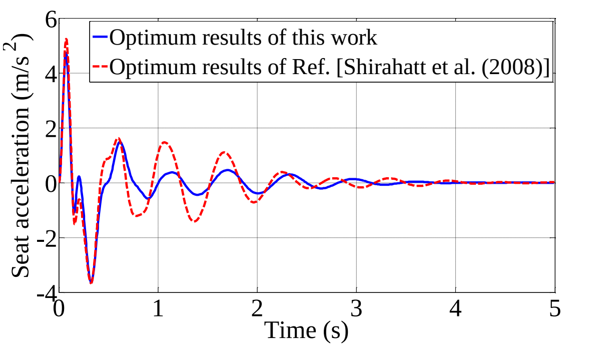

Fig. 9 Time responses of seat acceleration of points Z_1 and *W*

Table 3 The values of objective functions and their associated design variables of the optimum points and point W

	F_1	F_2	$k_1=k_2$	$k_3=k_4$	$c_1=c_2$	$c_3=c_4$	k_p	c_p
X_1	4.358	39510	76400	51318	1256	2104	93343	884
Y_1	5.698	39042	91079	64408	2817	2966	117078	416
Z_1	4.737	39152	79879	64407	2700	2856	94838	776
X_2	4.274	6.984	75284	57104	1007	2560	90251	846
Y_2	5.516	6.026	95749	66402	2901	2882	109505	557
Z_2	4.587	6.269	76715	57915	2595	2715	91651	795
X_3	4.397	0.1963	76170	63998	1159	2418	94950	827
Y_3	5.417	0.1599	96088	62794	2826	2942	110956	692
Z_3	4.639	0.1731	76415	63016	2701	2447	93657	807
X_4	2.053	39539	79554	33210	1080	2224	118190	577
Y_4	3.019	39068	95713	56587	2819	2873	100082	830
Z_4	2.540	39253	80903	38259	2646	2696	116515	801
X_5	4.446	39572	76586	47248	1962	906	112813	747
Y_5	5.532	39041	96359	67602	2916	2729	100698	660
Z_5	4.925	39258	77798	56863	2872	1959	108363	723
X_6	3.276	3.688	78324	41024	1773	928	94015	844
Y_6	3.916	2.998	89158	65163	2951	2938	104190	841
Z_6	3.579	3.175	78601	41345	2949	2408	95958	694
W			96861	52310	2460	2281	98935	615

Table 4 Values of objective functions of optimum point W

	SA	PA	RA	TF	TV	SD
Point W	5.2355	2.9660	5.4177	39246	6.4802	0.1758

Table 5 Maximum absolute value of seat acceleration of optimum points and their improvement percentage

	$Max\lvert\ddot{\delta}_p\rvert$	Improvement percentage
W	5.235	
Z_1	4.737	10%
Z_2	4.587	12%
Z_3	4.638	11%
Z_4	5.137	2%
Z_5	5.055	3%
Z_6	4.870	7%

Also, the time behavior of the other objectives corresponding to optimum values of point Z_1 and the optimum values proposed in Shirahatt *et al.* (2008) are shown for the sake of comparison in Figs. 10-14. Here, for plotting the Figs. 12-14, the value of tire force, tire velocity and suspension deflection of whole vehicle are equalized to the sum value of absolute of function values in wheels, as follows

$$F^D = \sum_{i=1}^{4} \left| F_i^D \right|, \; i = 1,2,3,4, \tag{21}$$

where F^D and F_i^D *(i=1,2,3,4)* are derived function value of whole vehicle and each wheel, respectively.

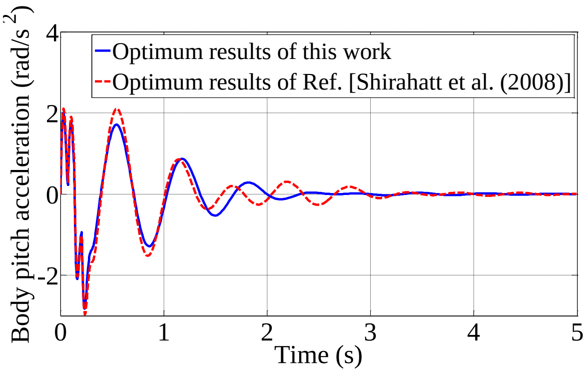

Fig. 10 Time responses of body pitch acceleration of points Z_1 and W

What is evident from these figures is that the values of the other objectives of the design point obtained from point Z_1 in the present study are also better than those corresponding with the design point given in Shirahatt *et al.* (2008). In Figs. 10-14, the maximum absolute value of body pitch acceleration, body roll acceleration, and derived dynamic tire force, tire velocity and suspension deflection of whole vehicle are improved from point *W* to Z_1 about 5%, 2%, 5%, 8% and 11% respectively. According to derived results, point Z_1 and other derived optimum points in this research are superior to results obtained by Shirahatt *et al.* (2008).

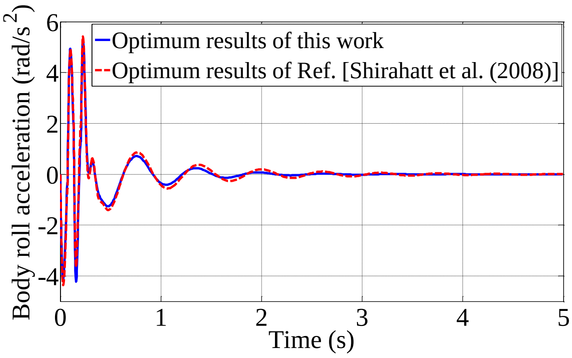

Fig. 11 Time responses of body roll acceleration of points Z_1 and *W*

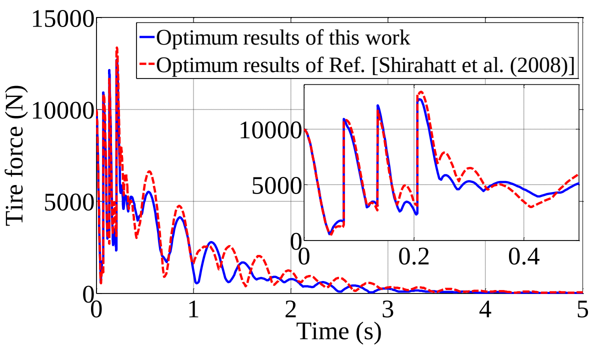

Fig. 12 Time responses of dynamic tire force of points Z_1 and *W*

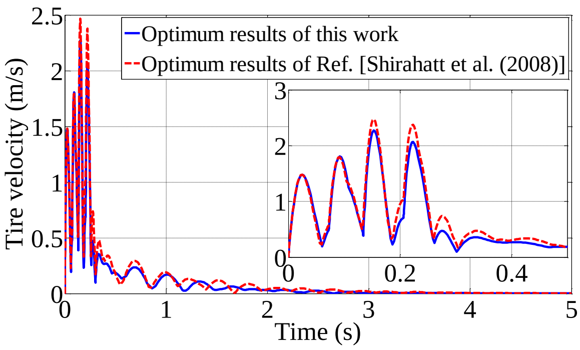

Fig. 13 Time responses of tire velocity of points Z_1 and *W*

When a dynamic system is excited by a suddenly applied nonperiodic excitation, the system response is transient and steady-state oscillations are generally not produced. In this condition, the system oscillates at its natural frequencies whose amplitude of vibration only depends on the type of excitation (Thomson and Dahleh 1998). If periodic function is applied for road profile to excite three dimensional vehicle models, the maximum value of objective functions takes place in steady-state response and the optimization results depend on amplitude and frequency of considered road profile. In this research, step function has been applied for road profile whose system response is only transient; hence, the maximum value of objective functions and the optimization results are independent from excitation frequency of road profile. Therefore, trade-off design points obtained in this research are applicable for any type of road profile. The natural frequencies of the present vehicle model with design variable ranges in Table 2 are about 1-10 Hz. In this regard, to show the comprehensiveness of the results of this research, time response of the model excited by various road profile frequencies has been investigated. Shirahatt *et al.* (2008) has applied two successive sinusoidal bumps with height $h=0.05\ m$ and wavelength $\lambda=20\ m$ for road profile to excite the eight-DOF vehicle model with velocity $v=20\ m/s$ as shown in Fig. 15. This road profile excites the model at a frequency of 1 Hz. The model in this research has been excited by this road profile and the same time delay which were applied for the step function has been used between tires. The time behavior of the seat acceleration for present eight-DOF vehicle model excited by this road profile corresponds to the optimum values of point Z_1along with optimum point *W* proposed in Shirahatt *et al.* (2008), are shown for the sake of comparison in Fig. 16. Also, the model has been excited by ten successive sinusoidal bumps with height $h=0.05\ m$ and wavelength $\lambda=0.4\ m$ (excitation frequency 50 Hz) as shown in Fig. 17. The time behavior of the seat acceleration for the model excited by this road profile corresponds to optimum values of point Z_1along with optimum point *W* are shown in Fig. 18.

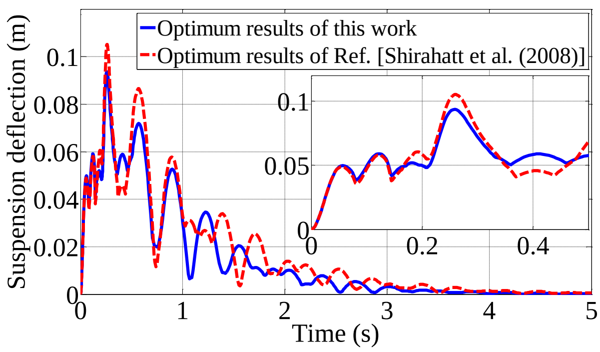

Fig. 14 Time responses of suspension deflection of points Z_1 and *W*

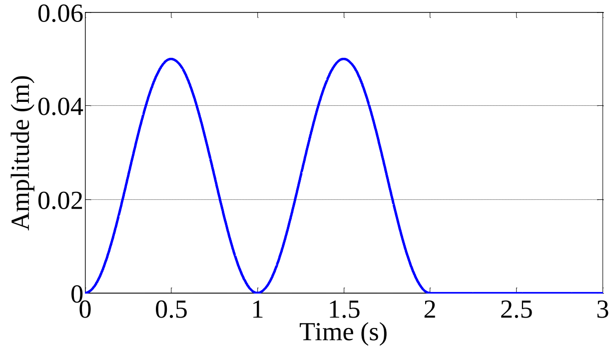

Fig. 15 Excitation shape created by low frequency sinusoidal road profile

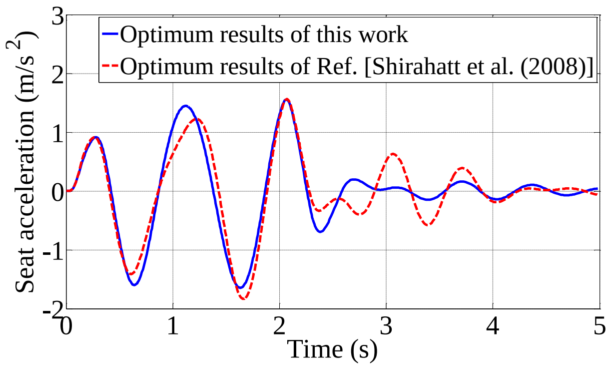

Fig. 16 Time responses of seat acceleration of points Z_1 and *W*

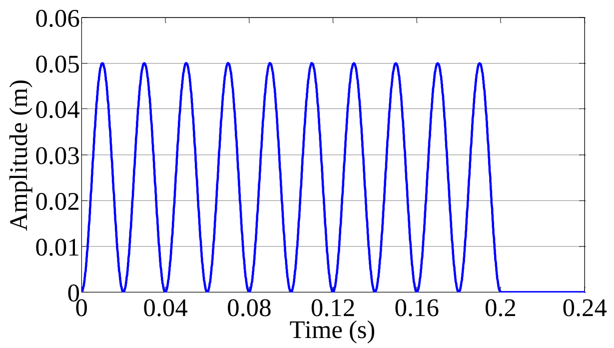

Fig. 17 Excitation shape created by High frequency sinusoidal road profile

In both Figs. 16 and 18, the maximum absolute value of seat acceleration are improved from point *W* to Z_1 about 10%. These figures clearly indicate that even with applying the sinusoidal shape for road profile and various excitation frequency, the derived values of seat accelerations via the design point obtained in the present research are better than those using the design point given in Shirahatt *et al.* (2008) and the results in this research are comprehensive for all vibration conditions.

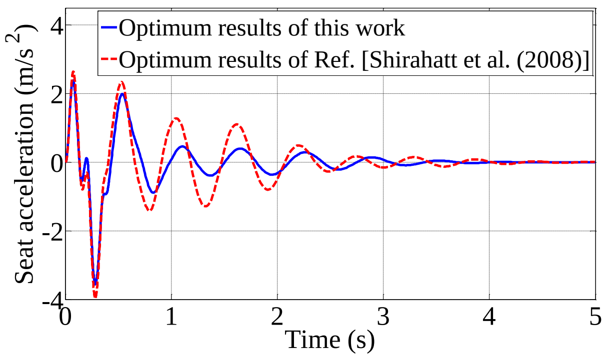

Fig. 18 Time responses of seat acceleration of points Z_1 and *W*

7. Conclusions

A Non-dominated sorting genetic algorithm II (NSGA-II) was employed to optimally design the full vehicle vibration model. Two objective groups, being in conflict with each other, were selected as ride comfort group and ride safety group. The ride comfort group consists of passenger seat acceleration, body pitch acceleration and body roll acceleration, and ride safety group comprises dynamic tire force, tire velocity and suspension deflection. With these ride parameters, objectives of the three dimensional vehicle models were also considered. A special optimizing technique combining weighted sum method and Pareto optimization was applied to transform Pareto double-objective optimization to Pareto full-objective optimization which can minimize all objectives, simultaneously. The Pareto front obtained from this weighted sum Pareto optimization method has minimized the full set of ride parameters of three dimensional vehicle model as objective functions, simultaneously. The results were derived from Pareto double-objective optimization and Pareto full-objective optimization which minimize pair objective and full objective respectively. It was shown that the unique trade-off design points in full-objective Pareto front can be selected minimizing weighted sum comfort parameters versus weighted sum safety parameters. A step function was used for road profile and was shown that, with such excitation form, optimum results are independent of excitation frequency. The comparison of the obtained optimum design points with those reported in the literature revealed the superiority and comprehensiveness of the results of the present research. For example, the optimum design point Z_6 was derived which can minimize all conflicting ride parameters of three dimensional vehicle model, simultaneously. Such three dimensional vehicle model and the multi-objective optimization of this model could obtain very important design points between conflicting objective functions.

Acknowledgments

This research work is supported by the Malek-Ashtar University of Technology of Iran. The authors are grateful to Innovative Research Team in School of Mechanical Engineering of ShahinShahr for their support in this work.

References

Barbosa, R.S. (2011), "Vehicle dynamic response due to pavement roughness", *J. Braz. Soc. Mech. Sci. Eng.*, **33**(3), 302-307.

Bharti, P.S., Maheshwari, S. and Sharma C. (2012), "Multi-objective optimization of electric-discharge machining process using controlled elitist NSGA-II", *J. Mech. Sci. Technol.*, **26**(6), 1875-1883.

Busch, J. and Bestle, D. (2014), "Optimisation of lateral car dynamics taking into account parameter uncertainties", *Vehicle Syst. Dyn.*, **52**(2), 166-185.

Chen, S., Wang, D., Chen, J., Liu, B. and Li, C. (2013), "Optimization of car sound package with statistical energy analysis model using grey relational analysis and taguchi method", *Fluct. Noise Lett.*, **12**(1), 1250024-1-1250024-20.

Costas, M., Díaz, J., Romera, L. and Hernández, S. (2014), "A multi-objective surrogate-based optimization of the crashworthiness of a hybrid impact absorber", *International Journal of Mechanical Science*, **88**, 46-54.

Deb K. (2001), *Multi-Objective Optimization using Evolutionary Algorithms*, John Wiley & Sons, Ltd.

Gu, X., Sun, G., Li, G., Huang, X., Li, Y. and Li, Q. (2013), "Multi objective optimization design for vehicle occupant restraint system under frontal impact", *Struct. Multidiscip. O.*, **47**(3), 465-477.

Gündoğdu, Ö. (2007), "Optimal seat and suspension design for a quarter car with driver model using genetic algorithms", *Int. J. Ind. Ergonom*., **37**(4), 327-332.

Hada, M.K., Menon, A. and Bhave, S.Y. (2007), "Optimisation of an active suspension force controller using genetic algorithm for random Iinput", *Defence Sci. J.*, **57**(5), 691-706.

Ihsan, S.I., Faris, W.F. and Ahmadian M. (2008), "Analysis of control policies and dynamic response of a Q-car 2-DOF semi active system", *J. Shock Vib.*, **15**(5), 573-582.

Jin, L., Yu, Y. and Fu, Y. (2016), "Study on the ride comfort of vehicles driven by in-wheel motors", *Adv. Mech. Eng*., **8**(3), 1-9.

Li, Z., Zheng, L., Ren, Y., Li, Y. and Xiong, Z. (2018), "Multi-objective optimization of active suspension system in electric vehicle with In-Wheel-Motor against the negative electromechanical coupling effects", *Mech. Syst. Signal Pr.*, **116**(2019), 545-565.

Liang, Y.J. and Wu, S.L. (2013), "Optimal vibration control for tracked vehicle suspension systems", *Math. Probl. Eng.*, 178354-1-178354-7.

Lin, C., Gao, F. and Bai, Y. (2018), "An intelligent sampling approach for metamodel-based multi-objective optimization with guidance of the adaptive weighted-sum method", *Struct. Multidiscip. O.*, **57**(3), 1047-1060.

Mahmoodabadi, M.J., Farhadi, F. and Sampour, S. (2018), "Firefly algorithm based optimum design of vehicle suspension systems", *Int. J. Dynam. Control*.

Panzade, P.K. (2005), "Modeling and Analysis of full vehicle for ride and handling", M.E. Thesis, PSG College of Technology, Coimbatore.

Sedighizadeh, M., Faramarzi, H., Mahmoodi, M.M. and Sarvi, M. (2014), "Hybrid approach to FACTS devices allocation using multi-objective function with NSPSO and NSGA-II algorithms in Fuzzy framework", *Int. J. Elec. Power Energ. Syst.*, **62**, 586-598.

Seifi, A., Hassannejad, R. and Hamed, M.A. (2015), "Optimum design for passive suspension system of a vehicle to prevent rollover and improve ride comfort under random road excitations", *Proceedings of the Institution of Mechanical Engineers, Part K: Journal of Multi-body Dynamics*, **230**(4), 426-441.

Shirahatt, A., Prasad, P.S.S., Panzade, P. and Kulkarni, M.M. (2008), "Optimal design of passenger car suspension for ride and road holding", *J. Braz. Soc. Mech. Sci. Eng*., **30**(1), 66-76.

Shojaeefard, M.H., Khalkhali, A., Faghihian, H. and Dahmardeh, M. (2017), "Optimal platform design using non-dominated sorting genetic algorithm II and technique for order of preference by similarity to ideal solution; application to automotive suspension system", *Engineering Optimization*, **50**(3), 471-482.

Thomson W.T. and Dahleh, M.D. (1998), *Theory of Vibration with Applications*, (5th Ed.), Upper Saddle River, NJ: Prentice Hall.

Tong, W. and Guo, K.H. (2012), "Simulation testing research on ride comfort of vehicle with global-coupling torsion-elimination suspension", *Phys. Procedia*, **33**, 1741-1748.

Uys, P.E., Els, P.S. and Thoresson, M. (2007), "Suspension settings for optimal ride comfort of off-road vehicles travelling on roads with different roughness and speeds", *J. Terramechanics*, **44**(2), 163-175.

Zhang, Y., Liu, G., Wang, P. and Karimi H. R. (2013), "Finite frequency vibration control for polytopic active suspensions via dynamic output feedback", *Math. Problem. Eng.*, 598489-1-598489-12.

CC